J Appl Electrochem (2014) 44:719–725
DOI 10.1007/s10800-014-0688-9

RESEARCH ARTICLE

Application of attapulgite/maltose system on mesoporous carbon material preparation for electrochemical capacitors

Xia Zhao · Heming Luo · Kaifa Du · Fengbo Zhang · Yabin Li

Received: 17 December 2013 / Accepted: 17 March 2014 / Published online: 30 March 2014

Abstract Mesoporous carbon materials were prepared through atmospheric pressure impregnation at room temperature using attapulgite as hard template and maltose as carbon source. N_2 absorption–desorption, X-ray diffraction, and transmission electron microscopy were used to determine the construction and morphology of the materials. The results showed that the prepared carbon materials possessed chain-layered structures whose surfaces were filled with ample nanoscale apertures. The materials also exhibited partial fasciculus with specific surface area and total pore volume of 628.6 $m^2\ g^{-1}$ and 1.31 $cm^3\ g^{-1}$, respectively. Constant current charge/discharge, cyclic voltammetry, and AC impedance tests were performed to evaluate the electrochemical performance of the materials. The constant current charge/discharge tests showed that the materials have excellent energy storage capacity. When the current density was 600 mA g^{-1}, the specific capacitance value reached 171 F g^{-1}. The materials showed quasi-rectangular features of typical cyclic voltammetry curve even at high scan rate (200 mV s^{-1}), indicating that they possess excellent rate capacity. The AC impedance tests showed that the materials were typical porous electrode materials with combination resistance of 0.82 Ω. The specific capacitance of the materials reached 79 % after 1,000 constant current charge/discharge cycles, indicating that they have superior cyclic stability.

Keywords Attapulgite · Maltose · Atmospheric pressure impregnation · Mesoporous carbon materials · Electrochemical performance

X. Zhao (✉) · H. Luo · K. Du · F. Zhang · Y. Li
College of Petrochemical Technology, Lanzhou University of Technology, Lanzhou 730050, China
e-mail: zhaoxia@lut.cn

1 Introduction

With the increase in energy consumption, particularly fossil energy, developing new energy resources has become a key factor in facilitating social and economic development. As a result, significant attention is being given to the development of highly efficient and environmentally friendly energy-storage devices. Electrochemical capacitors (ECs) or supercapacitors are new energy-storage and transmission devices. Compared with a traditional capacitor, an EC has relatively high energy density and power density, as well as excellent cycling stability [1–5]. The performance of an EC is significantly affected by the properties of its electrode materials. ECs can be classified based on their corresponding electrode materials, namely, electric double-layer, metallic oxide, and conductive polymer-based Faraday pseudocapacitors.

Carbon materials are used in various fields, such as absorption, catalysis, and energy storage, because of their large specific surface area, as well as their physical, chemical, and thermal stabilities [5–10]. Preparation of porous carbon material includes activation processes that are conducted through template-based methods that produce carbon materials with adjustable aperture structures. Some Si-based molecular sieves, artificial zeolites, and metallic oxides are used as aperture modifiers to control the structures of porous carbon materials. The common templates include SBA-15 [11], MCM-48 [12], KIT-6 [13], zeolite [14–17], MgO [18], and $Ni(OH)_2$/NiO [19]. However, the preparation of porous carbon materials is relatively expensive, thereby restricting their large-scale application.

Attapulgite is a common natural porous mineral that exhibits strong absorption capacity. It is often used in various applications, such as absorption and catalysis.

Studies on porous carbon materials prepared with the use of attapulgite as hard template have mainly focused on the formation of aperture structure, but studies on the electrode performance of prepared porous carbon materials are relatively rare. Peng et al. [20] used attapulgite as template and furfural alcohol as a carbon source to obtain porous carbon materials, after which they prepared polypyrrole/porous carbon composite electrode material through in situ polymerization. In the present study, we used maltose as the carbon source and attapulgite as the template to obtain porous carbon materials through atmospheric pressure impregnation and carbonization. Constant current charge/discharge tests under different current densities, cyclic voltammetry test at different scan rates, and electrochemical AC impedance test were conducted to evaluate the electrochemical performance of the products.

2 Materials and methods

2.1 Preparation of mesoporous carbon materials

A standard sieve was used to obtain templates (attapulgite) with certain particle sizes, which were then treated with acid and dried in vacuum for 24 h at 80 °C. The template, maltose, deionized water, and sulfuric acid were weighed to obtain a certain mass ratio for impregnation and filtering at room temperature. The filtrate was then placed in a box furnace and heated to 100 °C for 4 h under N_2 atmosphere. The temperature was increased to 150 °C for 6 h and to certain temperatures (600, 700, 800, and 900 °C) for 3 h. HF (10 wt%) was used to treat template/carbon compounds, which were then washed and dried to obtain the mesoporous carbon materials. The obtained materials were labeled *AMC*-18(6)-*X*-3, (*A*, *M*, *C*, and *X* denote attapulgite, maltose, carbon materials, and carbonization temperature, respectively.)

2.2 Preparation of mesoporous carbon electrode

One drop of PTEE (0.5 mg) as binder and some absolute ethyl alcohol as dispersant were added to 5 mg mixture of the as-prepared mesoporous carbon materials, graphite, and acetylene black (8:1:1) to prepare the mash, which was then uniformly coated on the nickel foam. The coated foam was dried in vacuum at 80 °C for 12 h, repressed for 1 min to 2 min under 10 MPa pressure, and then dried in vacuum for 6 h.

2.3 Morphological analysis and electrochemical testing of mesoporous carbon electrode materials

The morphology and structure of the materials were elucidated through transmission electron microscopy (TEM, Tecnai-G2, FEI), X-ray diffraction (XRD, D/Max-2400) (RINT-2000, Rigaku), and N_2 absorption/desorption testing (Tristar II 3020, Micromeritics Instrument Corp.). A conventional three-electrode system containing 2 mol L^{-1} KOH solution as electrolyte was used in the electrochemical measurements, with porous carbon electrode, platinum sheet, and SCE as working electrode, auxiliary electrode, and reference electrode, respectively. The charge/discharge, cyclic voltammetry, and AC impedance behavior tests were conducted using an electrochemical workstation (CHI660D, Shanghai Chenhua Instrument Company). The working electrodes were soaked in electrolyte for 12 h before the tests.

3 Results and discussion

3.1 Construction and morphology analysis

3.1.1 TEM analysis

AMC-18(6)-700-3 are chain-layer carbon materials with ample aperture structures that are generally disordered. In this study, the obtained materials showed fasciculus structures with surfaces that partially contained abundant open-aperture structures (Fig. 1a–d). In addition, the disordered accumulation of materials formed a vast accumulated space that resulted in relatively high specific surface area and pore volume. The pore size distribution was concentrated in the range of 2 nm to 50 nm with few micropores and macropores.

3.1.2 Brunauer–Emmett–Teller (BET) analysis

Hysteresis was observed in the N_2 absorption/desorption isotherms (Fig. 2a), indicating that the curve belongs to type IV isotherms and that ample mesoporous structures exist in the AMC-18(6)-700-3 structure. Furthermore, when the relative pressure $p/p^0 < 0.1$, the absorbing capacity of the materials gradually increased with the increasing relative pressure, indicating that certain amounts of micropores exist in the materials. We speculate that the micropores were generated through the following three routes: carbonization of carbon precursor, reverse replication of the template, and accumulation of chain-layer carbon materials. When p/p^0 was approximately 0.4, capillary condensation occurred, forming a pore size of 4 nm. When the relative pressure $p/p^0 = 1$, absorption quality remarkably increased because of the absorption effect of large-aperture channels [21]. The material pore size distribution mainly centered within 2–20 nm and mainly focused on 3.5 and 12 nm (Fig. 2b), consistent with the results in Fig. 2a. The pore structural parameters of *AMC*-18(6)-700-3 are

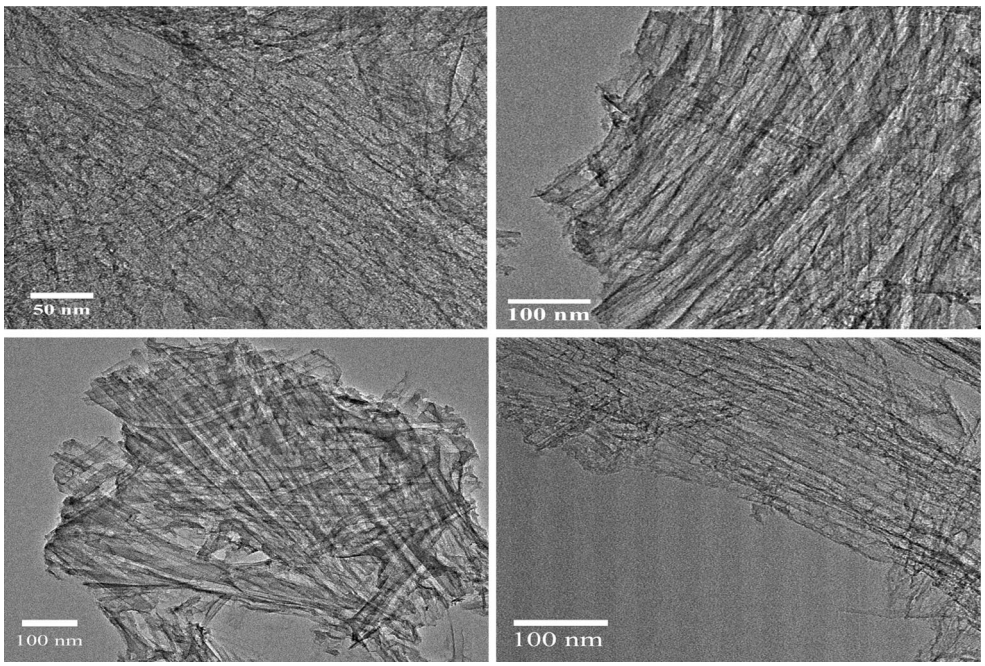

Fig. 1 The TEM *images* of AMC-18(6)-700-3

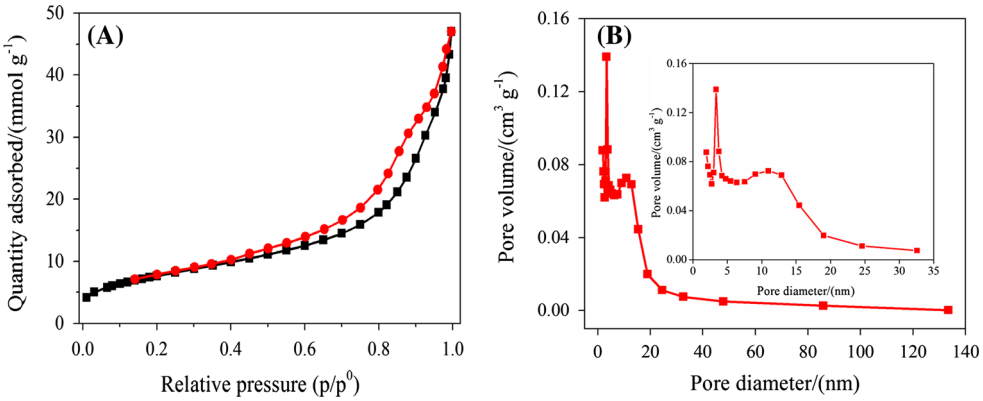

Fig. 2 The N_2 adsorption and desorption isotherms (**a**) and the pore size distribution *curves* (**b**) of AMC-18(6)-X-3

Table 1 Characterization pore Structure of AMC-18(6)-700-3

Sample	S_{BET} (m^2 g^{-1})	V_{total} (cm^3 g^{-1})	V_{micro} (cm^3 g^{-1})	V_{meso} (cm^3 g^{-1})	V_{meso}/V_{total} (%)	Average pore diameter (nm)
AMC-18(6)-700-3	628.6	1.31	0.22	1.09	83.2	8.33

described in Table 1, where the mesoporous porosity reached 83 % and the microporous pore volume was 0.22 cm^3 g^{-1}. Relatively high mesoporous porosity and abundant micropores are important in improving energy storage ability.

In accordance with the BET formula, S_{BET} is obtained by adopting absorption branch statistics; V_{total} is calculated from the absorbing capacity of liquid nitrogen when p/p^0=0.97; V_{micro} is calculated from the absorbing capacity of liquid nitrogen when $p/p^0 = 0.1$; and $V_{meso} = V_{total}–V_{micro}$.

3.1.3 XRD analysis

The mesoporous carbon materials prepared at different carbonization temperatures shared the same crystalline structures (Fig. 3). The wide "bread peak" and low-intensity diffraction peak, which appeared at $2\theta \approx 21°$ and 43°, correspond to two characteristic diffraction peaks of graphite, namely, (002) and (101). These peaks indicated that the pore carbon materials possessed graphitic and amorphous structures. The structures were beneficial to

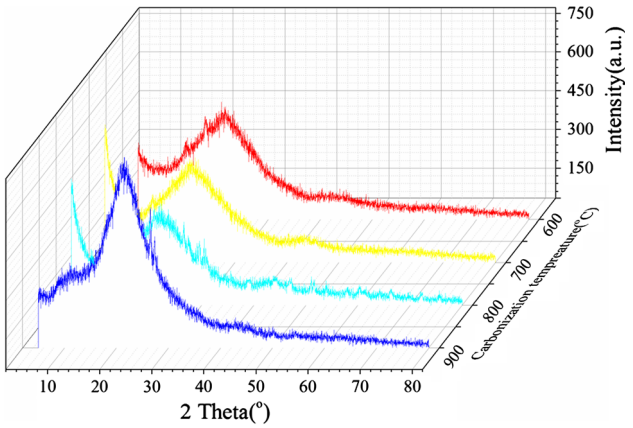

Fig. 3 The XRD patterns of mesoporous carbon materials prepared at different carbonization temperatures

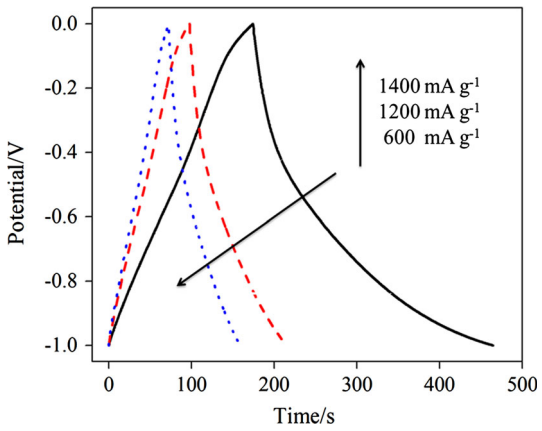

Fig. 5 The constant current charge/discharge *curves* of AMC-18(6)-700-3 electrode at different current densities

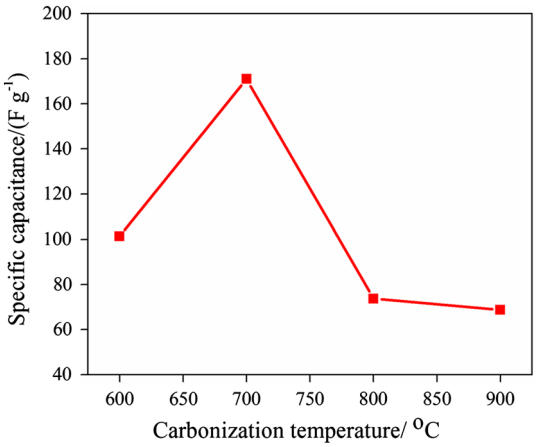

Fig. 4 The specific capacitance of AMC prepared at different carbonization temperatures

electrolyte ion permeation into the inner material, resulting in improved electrochemical performance of the materials. In addition, the diffraction peak intensities [i.e., (002) and (001)] of the carbon materials were enhanced with increasing carbonization temperature, indicating that high-temperature treatment is beneficial in improving the degree of graphitization of the material.

3.2 Electrochemical test

3.2.1 Constant current charge/discharge

The specific capacitance of *AMC*-18(6)-*X* at 600 mA g^{-1} current density is shown in Fig. 4. The specific capacitance is calculated using Eq. (1).

$$C = \frac{i \times \Delta t}{m \times \Delta E}, \quad (1)$$

where C (F/g) is the specific capacitance, i (mA) is the charge/discharge current, t(s) is the discharge time, m (g) is the mass of active material, and E (V) is the voltage window.

Figure 4 also shows that the specific capacitance first increased, and then decreased with the increase in carbonization temperature. When the carbonization temperature was 700 °C, the electrode exhibited the maximum specific capacitance of 171 F g^{-1}. When the carbonization temperature elevated from 600 °C to 800 °C, the specific capacitance increased from 101–171 F g^{-1}, and then decreased sharply to 74 F g^{-1} with an attenuation rate of 56.7 %. This phenomenon can be attributed to the incomplete carbonization of the predecessor. The inferior pore structures and low degree of graphitization contributed to the low conductivity and inferior electrochemical performance at low carbonization temperature. At high carbonization temperature, the skeleton of carbon materials shrunk, leading to the formation of a pore wall and channel collapse after the template was removed. The foregoing resulted in specific surface area reduction, weakening of the double electrode-layer effect, and attenuation of specific capacitance. The specific capacitance hardly decreased with the increase in temperature to 900 °C. We can infer that the degree of graphitization and conductivity increased with the increase in carbonization temperature, which resulted in specific capacity attenuation caused by the decrease in specific surface area.

The constant current charge/discharge curves of the *AMC*-18(6)-700-3 electrode at different current densities are presented in Fig. 5. The discharge time decreased gradually with the increase in current density because the electrolyte ion can completely infiltrate the inner channel of the electrode materials and form a double electric-layer structure at the interface between electrolyte and active materials at low current density. In addition, the electrolyte ion cannot fully wet the channel of the materials to form a double layer at high discharge current, reducing the

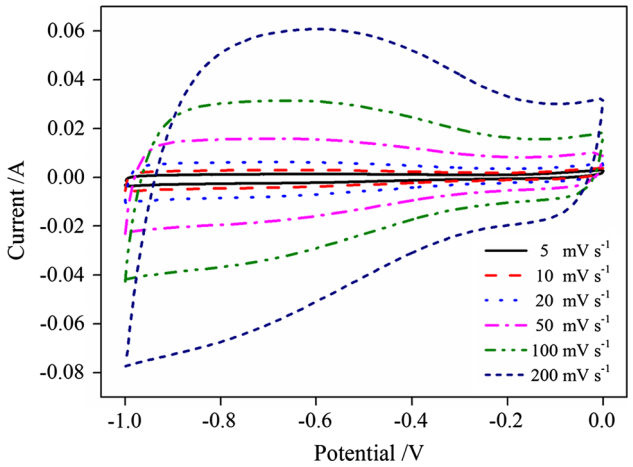

Fig. 6 The cyclic voltammograms for electrode AMC-18(6)-700-3 at various scan rates

utilization rate of materials and consequently shortening the discharge time. When the current density was 600 mA g^{-1}, the charge/discharge curve exhibited the "trailing" phenomenon, which indicated that the material possessed a microporous structure.

3.2.2 *Cyclic voltammetry*

The cyclic voltammetry curves of the *AMC*-18(6)-700-3 electrode at scan rates of 5, 10, 20, 50, 100, and 200 mV·s^{-1} are shown in Fig. 6. The cyclic voltammetry curves showed quasi-rectangular features of a double electric-layer EC cyclic voltammogram with bulging parts from −0.4 V to −1 V [15], as well as rapid current response characteristics. When the scan rate reached 200 mV s^{-1}, the curve maintained the quasi-rectangular features to some extent, indicating the excellent circulation percentage of the materials and the existence of mesopores and macropores in the material structures. Moreover, the specific capacitance decreased with the increase in scan rate because the electrolyte ion cannot enter the inner channel, thereby weakening the double electric-layer effect and then decreasing the utilization rate of the specific surface area of materials.

3.2.3 *Electrochemical impedance*

The electrochemical impedance spectra of the *AMC*-18(6)-*X*-3 at open-circuit voltage with frequency area of 0.01–10^5 Hz and oscillating voltage of 5 mV are shown in Fig. 7a. The mesoporous carbon electrode materials exhibited almost no obvious arc in the high-frequency area, indicating that the contact resistance on the interface between the material and the electrolyte solution was relatively small. The intercept between curves in the high-frequency and real axis (Z') represented combination resistance, which is relevant to its nature, as well as contact among electrolyte, carbon material, and current collector. The combination resistance values of the as-prepared materials were 0.68 Ω (600 °C), 0.64 Ω (700 °C), 0.79 Ω (800 °C), and 0.78 Ω (900 °C). The curve was nearly perpendicular to the real axis in the low-frequency area, indicating that the materials possessed the pure capacitance behavior of an ideal EC. However, the curves also deflected from the imaginary axis (Z''), demonstrating the existence of frequency dispersion effect [10]. Based on the constant current charge/discharge results, we studied the frequency response characteristics of the carbon materials prepared at 700 °C. As shown in Fig. 7b, the straight line with 45 slope in the middle–low-frequency area represents Warburg resistance, which is due to ion spreading from the inner electrode materials and electrolyte to the electrode surface; the length represents the value of ion diffusion resistance [9, 22]. *AMC*-18(6)-700-3 had small Warburg resistance. The "break frequency" reflected the rapid charge/discharge performance of the materials. *AMC*-18(6)-700-3 also exhibited outstanding rapid charge/discharge performance and reached "charge saturated conditions" easily [9, 23].

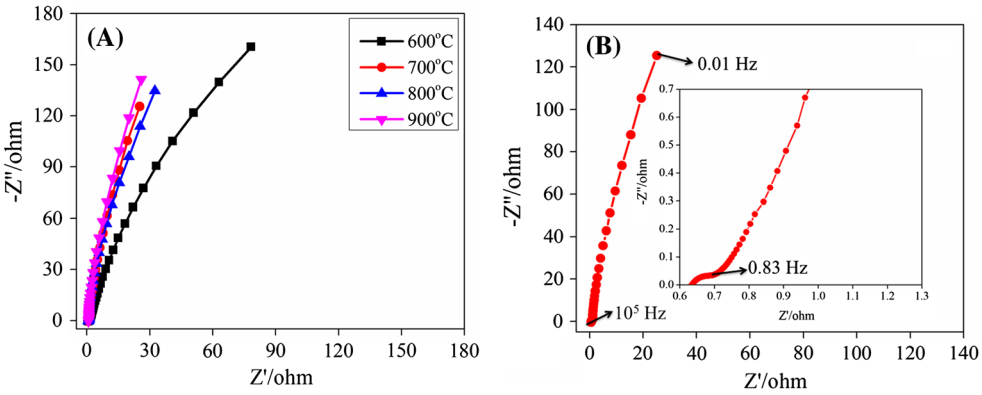

Fig. 7 **A** The electrochemical impendence spectra of AMC (*a*) and AMC-18(6)-700-3 (*b*) (Insert: magnified high-frequency area). **B** The electrochemical impendence spectra of AMC (*a*) and AMC-18(6)-700-3 (*b*) (*Inset* magnified high-frequency area)

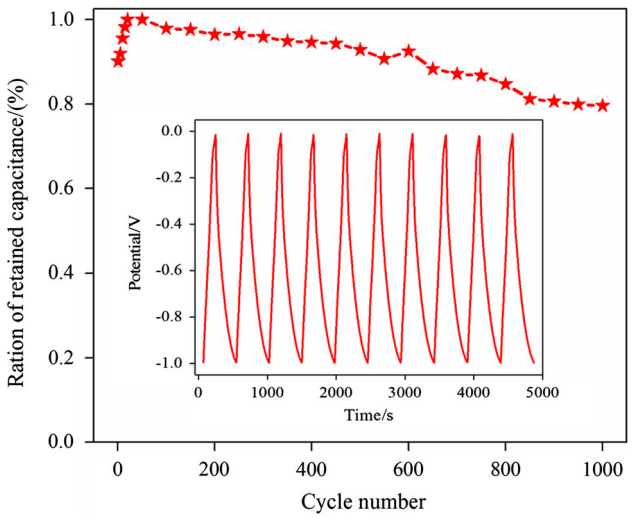

Fig. 8 Cycle life of the AMC-18(6)-700-3 electrode at the current density of 600 mA g. And the inset is the first 10 cycles of CCD *curves*

3.2.4 Cycle life

The cycle life of the electrode at 600 mA g^{-1} current density under the potential window of −1 to 0 V was determined (Fig. 8). The specific capacitance increased remarkably at the first stage of cycle because the contact performance between the porous carbon materials and the electrolyte improved gradually with the charge/discharge cycles, which resulted in complete wetting of the materials. As shown in Fig. 8, the electrode *AMC*-18(6)-700-3 exhibited maximum specific capacitance at the 20th constant current charge/discharge cycle. The specific capacitance started to decrease after the 50th cycle and reached a stable condition without obvious attenuation after the 850th cycle. Compared with the 20th cycle, the capacitance retention rate reached 79 % after 1,000 consecutive charge/discharge cycles.

4 Conclusions

We used attapulgite as template and maltose as carbon source to reduce the preparation cost of porous carbon materials.

Disordered stacking structures with specific surface area of 628.6 m^2 g^{-1} and total pore volume and mesoporous porosity of 1.46 cm^3 g^{-1} and 83.2 %, respectively, were obtained through atmospheric pressure impregnation.

When the impregnation time was 18 h at 700 °C carbonization temperature, the resulting materials exhibited outstanding electrochemical performance. At 600 mA g^{-1} current density, the specific capacitance reached up to 171 F g^{-1}. The cyclic voltammetry curve maintained quasi-rectangular features with the increase in scan rate up to 200 mV s^{-1}. The AC impedance tests showed that the combination resistance of the materials was relatively small, with series resistance of 0.82 Ω.

The results of cyclic testing showed that the retention rate of specific capacitance reached 79 % after 1,000 consecutive current charge/discharge cycles.

Acknowledgments This work was supported by the Funds for Creative Research Groups of China (No. 51121062), the National Natural Science Foundation of China (5126803), the College Students Training Project for Creative and Entrepreneurship of China (121073115), the Research Project for Education Department of Gansu Province (1205ZTC032), and the Excellent Young Teachers in Lanzhou University of Technology Training Project (1005ZCX016).

References

1. Zhu YW, Murali S, Stoller MD, Ganesh KJ, Cai WW, Ferreira PJ, Pirkle A, Wallace RM, Cychosz KA, Thommes M, Su D, Stach EA, Ruoff RS (2011) Carbon-based supercapacitors produced by activation of graphene. Science 332(6037): 1537–1541
2. Chmiola J, Largeot C, Taberna PL, Simon P, Gogotsi Y (2010) Monolithic carbide-derived carbon films for micro-supercapacitors. Science 328(5977):480–483
3. El-Kady MF, Strong V, Dubin S, Kaner RB (2012) Laser scribing of high-performance and flexible graphene-based electrochemical capacitors. Science 335(6074):1326–1330
4. Zhang JT, Zhao XS (2012) On the configuration of supercapacitors for maximizing electrochemical performance. Chem Sus Chem 5(5):818–841
5. Wu ZS, Sun Y, Tan YZ, Yang SB, Feng XL, Müllen K (2012) Three-dimensional graphene-based macro and mesoporous frameworks for high-performance electrochemical capacitive energy storage. J Am Chem Soc 134(48):19532–19535
6. Xia YD, Yang ZX, Gou XL, Zhu YQ (2013) A simple method for the production of highly ordered porous carbon materials with increased hydrogen uptake capacities. Int J Hydrog Energy 38(12):5039–5052
7. Lee JS, Joo SH, Ryoo R (2002) Synthesis of mesoporous silicas of controlled pore wall thickness and their replication to ordered nanoporous carbons with various pore diameters. J Am Chem Soc 124(7):1156–1157
8. Borchardt L, Oschatz M, Lohe M, Presserb V, Gogotsib Y, Kaskel S (2012) Ordered mesoporous carbide-derived carbons prepared by soft templating. Carbon 50(11):3987–3994
9. Brun N, Prabaharan RS, Surcin C, Morcrette M, Deleuze H, Birot M, Babot O, Achard MF, Backov R (2012) Design of hierarchical porous carbonaceous foams from a dual-template approach and their use as electrochemical capacitor and li ion battery negative electrodes. J Phys Chem C 116(1):1408–1421
10. Korenblit Y, Rose M, Kockrick E, Borchardt L, Kvit A, Kaskel S, Yushin G (2010) High-rate electrochemical capacitors based on ordered mesoporous silicon carbide-derived carbon. ACS Nano 4(3):1337–1344
11. Liu HY, Wang KP, Teng H (2005) A simplified preparation of mesoporous carbon and the examination of the carbon accessibility for electric double layer formation. Carbon 43(3):559–566
12. Maiyalagan T, Nassr ABA, Alaje TO, Bron M, Scott K (2012) Three-dimensional cubic ordered mesoporous carbon (CMK-8) as

highly efficient stable Pd electro-catalyst support for formic acid oxidation. J Power Sources 211:147–153
13. Ania CO, Khomenko V, Raymundo-Piñero E, Parra JB, Béguin F (2007) The large electrochemical capacitance of microporous doped carbon obtained by using a zeolite template. Adv Funct Mater 17(11):1828–1836
14. Barata-Rodrigues PM, Mays TJ, Moggridge GD (2003) Structured carbon adsorbents from clay, zeolite and mesoporous aluminosilicate templates. Carbon 41(12):2231–2246
15. Nishihara H, Yang QH, Hou PX, Unno M, Yamauchi S, Saito R, Paredes JI, Martínez-Alonso A, Tascón JD, Sato Y, Terauchi M, Kyotani T (2009) A possible buckybowl-like structure of zeolite templated carbon. Carbon 47(5):1220–1230
16. Meyers CJ, Shah SD, Patel SC, Sneeringer RM, Bessel CA, Dollahon NR, Leising RA, Takeuchi ES (2001) Templated synthesis of carbon materials from zeolites (y, beta, and zsm-5) and a montmorillonite clay (k10): physical and electrochemical characterization. J Phys Chem B 105(11):2143–2152
17. Morishita T, Tsumura T, Toyoda M, Przepiórskic J, Morawskic AW, Konnod H, Inagakie M (2010) A review of the control of pore structure in MgO-templated nanoporous carbons. Carbon 48(10):2690–2707
18. Wang DW, Li F, Liu M, Lu GQ, Cheng HM (2008) 3D Aperiodic Hierarchical Porous Graphitic Carbon Material for High-Rate Electrochemical Capacitive Energy Storage. Angew Chem 120(2):379–382
19. Shi LM, Yao JF, Jian JL, Zhang LX, Xu NP (2009) Preparation of mesopore-rich carbons using attapulgite as templates and furfuryl alcohol as carbon source through a vapor deposition and furfuryl alcohol as carbon source through a vapor deposition polymerization method. Microporous Mesoporous Mater 122:294–300
20. Peng H, Mou JJ, Wang H, Wang AT, Ma GF, Lei ZQ (2012) Preparation of PPy/porous carbon composites by using palygorskite as template and its application in electrochemical capacitor electrode. The 16th Reactive Polymer Symposium, Lanzhou, p 219–220
21. Zhang XY, Wang XY, Su JC, Wang XY, Jiang LL, Wu H, Wu C (2012) The effects of surfactant template concentration on the supercapacitive behaviors of hierarchically porous carbons. J Power Sources 199:402–408
22. Gao Z, Yang WL, Wang J, Wang B, Li ZS, Liu Q, Zhang ML (2013) A new partially reduced graphene oxide nanosheet/polyaniline nanowafer hybrid as supercapacitor electrode material. Energy Fuel 27(1):568–575
23. Luo HM, Yang P, Zhang FB (2013) Preparation and electrochemical properties of coke powder activated carbon based electrode materials. J Mater Sci: Mater Electron 24:586–593